

Diverse fluctuations and anisotropic Grüneisen parameter behavior in iron-based superconductor $\text{Ba}(\text{Fe}_{1-x}\text{Co}_x)_2\text{As}_2$ and their correlation with superconductivity

Chiaki Fujii¹, Shalamujiang Simayi^{*}, Kouhei Sakano¹, Chizuru Sasaki¹, Mitsuteru Nakamura¹, Yoshiki Nakanishi^{1,4}, Kunihiro Kihou^{2,4}, Masamichi Nakajima^{2,4}, Chul-Ho Lee^{2,4}, Akira Iyo^{2,4}, Hiroshi Eisaki^{2,4}, Shin-ichi Uchida^{2,3,4}, and Masahito Yoshizawa^{†,4}

¹ *Graduate School of Engineering, Iwate University, Morioka 020-8551*

² *National Institute of Advanced Industrial Science and Technology (AIST), Tsukuba 305-8568*

³ *Graduate School of Science, The University of Tokyo, Tokyo 113-0033*

⁴ *Transformative Research-project on Iron Pnictides (TRIP), Japan Science and Technology Agency, Tokyo 102-0075*

March 15, 2022

Abstract

In this study, the temperature dependence of elastic constants C_{11} , C_{33} , $C_E = (C_{11} - C_{12})/2$, C_{66} and C_{44} of the iron-based superconductor $\text{Ba}(\text{Fe}_{1-x}\text{Co}_x)_2\text{As}_2$ (0 to 0.245) have been measured. This system shows a large elastic softening in C_{66} towards low temperatures. In addition to C_{66} , which originates from orthorhombic structural fluctuation, the samples near the optimal concentration show remarkable structural fluctuation in C_{11} and C_{33} elastic modes, which correspond to Γ_1 (C4) symmetry. It suggests the existence of diverse fluctuations in this system. Grüneisen parameters were analyzed under some assumptions for structural and magnetic transition temperatures. Results showed that the Grüneisen parameters for the inter-plane strain are remarkably enhanced toward the QCP, while those for the in-plane stress tend to turn down near the QCP. Grüneisen parameters for the superconducting transition are anisotropic and shows remarkable Co-concentration dependence, suggesting that the in-plane isotropic compression and inter-layer elongation enhance the superconductivity. The correlation of Grüneisen parameters between T_S , T_N and T_{sc} shows c -axis elongation and its relevant role in the emergence of superconductivity in this system.

^{*}Present address: Renewable Energy Research Center, AIST

[†]Present address: Faculty of Science, Osaka University

[‡]E-mail address: yoshizawa@iwate-u.ac.jp

Keywords: Elastic constant, Iron-based superconductor, BaFe₂As₂, Grüneisen parameter.

1 Introduction

Today, superconductors are widely used in daily life. Magnetic resonance imaging (MRI) working with superconducting magnet provides with high resolution image of human body, and a powerful tool for medical diagnosis. Superconducting quantum interference devices (SQUID) has been used for brain research and detection of diseases. Novel superconductors (SCs) with higher critical temperature T_{sc} will be desired for wider applications of SCs. In 2008, iron-based superconductor (SC) was discovered by Hosono Group at Tokyo Institute of Technology.[1] This new type of SC has been attracted much attention and promoted projects due to its relatively high superconducting transition temperature T_{sc} although it contains a magnetic ion Fe as a constitutional element.[2] Such high T_{sc} of iron-based SCs has not been brought about by phonon, but possibly by other mechanisms.[3] Therefore, it is expected that investigation of iron-based materials would lead to a discovery of novel SCs with higher T_{sc} .

One of the key strategies to investigate the superconductivity is quantum criticality. According to recent studies for oxide SCs and strong correlated SCs, the superconducting phases of these systems are located near the neighboring phases like magnetic order. These neighboring phases disappear towards quantum critical point (QCP) by tuning control parameters such as hydrostatic pressure, chemical doping and magnetic field, and superconductivity turns out. Figure 1 shows the phase diagram of Ba(Fe_{1-x}Co_x)₂As₂ (Ba122), which will be reported in this article. As can be seen in the Fig. 1, the structural transition temperature T_S of the parent compound BaFe₂As₂ is 134.4 K, and it gradually decreases by replacing Fe by Co. T_S gradually decreases to zero at the QCP ($x=0.07$), and where T_{sc} reached to the maximum value. These alternations of the phases such as structural, magnetic and superconducting one suggests the importance of the neighboring phase in the emergence of superconductivity in iron based superconducting system. Fluctuations of the neighboring phase possibly mediates superconductivity. This consideration would lead us to find out a new type of superconductivity through the systematic investigations of the order and its fluctuation of the neighboring phase. Iron-based SCs show magnetic and structural (orbital) phases near to the superconducting phase, therefore there are two proposals were objected for the superconducting mechanism of iron-based SCs, they are magnetic and orbital characters. Namely, spin fluctuations and orbital fluctuations are new probable candidates for the superconductivity of iron-based SCs.

Investigation on the order of the neighboring phases and the order parameter fluctuations would be crucial for the superconductivity research. Elastic constant measurements are very powerful tools to investigate structural fluctuations. Ultrasonic wave and elastic strain introduced into solid for the sound velocity measurements breaks the local symmetry of the crystal. Because, as illustrated in Fig. 2, these elastic strains have the same symmetry as the elastic quadrupoles (rank-2 multipoles), therefore they can couple with the orbital degrees of freedom. As a result, those elastic constants which are the strain susceptibilities provide the relevant informations on the orbitals.

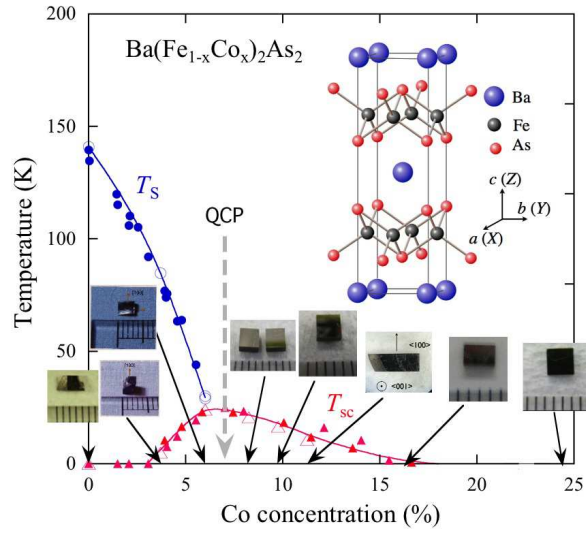


Figure 1: (Color online) Phase diagram and crystal structure of $\text{Ba}(\text{Fe}_{1-x}\text{Co}_x)_2\text{As}_2$. Crystal structure of BaFe_2As_2 belongs to the base-centered tetragonal crystal class $I4/mmm$. The adopted XYZ coordinates are described in the figure. These pictures of eight single crystals used in this experiment with their locations in the phase diagram are also shown in the figure. T_S and T_{sc} are the structural and superconducting phase transition temperatures. Open symbols are obtained by the previous work.[4] Closed symbols are reported in the previous studies.[5, 6]

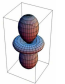

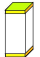
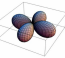
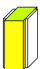
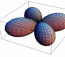
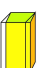
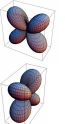


Symmetry D_{4h} $4/mmm$	orbitals, quadrupoles	elastic strain, deformation	elastic constants
Γ_1 A_{1g}	 $O_{zz} = \hat{Z}^2$ $d_{3z^2-r^2}$	 $\epsilon_{xx} + \epsilon_{yy}$  ϵ_{zz}	$\frac{1}{2}(C_{11} + C_{12})$ C_{33}
Γ_3 B_{1g}	 $O_x^2 = \hat{X}^2 - \hat{Y}^2$ $d_{x^2-y^2}$	 $\epsilon_{xx} - \epsilon_{yy}$	$C_E = \frac{1}{2}(C_{11} - C_{12})$
Γ_4 B_{2g}	 $O_{xy} = \hat{X}\hat{Y}$ d_{xy}	 ϵ_{xy}	C_{66} $S_{66} = \frac{1}{C_{66}}$
Γ_5 E_g	 $O_{yz} = \hat{Y}\hat{Z}$ d_{yz} $O_{zx} = \hat{Z}\hat{X}$ d_{zx}	 ϵ_{yz}  ϵ_{zx}	C_{44}

Figure 2: (Color online) Orbitals, quadrupoles, elastic strains, and their corresponding elastic constants classified into the irreducible representation of the point group D_{4h} . Figure cited from M. Yoshizawa *et al.*, Mod. Phys. Lett. B **26** (2012) 1230011. ©2012, Modern Physics Letters B.

It has been reported that some iron-based SCs show large elastic anomalies at low temperatures. Thin shape samples of polycrystalline LaFeAsO, BaFe₂As₂ and BaFe_{1.84}Co_{0.16}As₂ show elastic softening towards low temperatures.[7, 8] Ultrasonic measurements for bulk samples have revealed that the elastic constant C_{66} of Ba(Fe_{1-x}Co_x)₂As₂ (Ba122) shows a remarkably large elastic softening.[9, 4] These anomalies are considered to be associated with the structural ordering of the neighboring phases. In other words, tetragonal crystal symmetry is broken and changed to orthorhombic one in the neighboring phase.

We have performed precise investigations of the elastic properties for Ba122, so far. Then, we found that the elastic compliance S_{66} ($=1/C_{66}$), a measure of structural fluctuation, behaves like the magnetic susceptibility near magnetic QCP, where it has been considered that spin fluctuation plays a relevant role for the emergence of superconductivity. These experimental facts suggest the fluctuations with the same symmetry of the strains participate in the emergence of superconductivity. These experimental studies have stimulated the interest of theoreticians. On the origin of the elastic anomaly, Fernandes *et al.* argued that the elastic anomalies are ascribed to nematic spin fluctuation.[8] Kontani *et al.* proposed orbital origin of the large elastic anomalies.[10, 11]

These previous works suggest that the elastic constants are a suitable tool to investigate the fluctuations existing in iron-base SCs. In our previous papers, it has been reported that the elastic constants of C_{33} and C_{66} of Ba122 system showed an elastic anomaly behavior near the QCP. According to our recent works, Fe(Se_{1-x}Te_x) shows elastic anomalies in elastic constants C_{11} , C_{44} , $(C_{11} - C_{12})/2$ in addition to C_{66} , and SrFe₂(As_{1-x}P_x)₂ exhibits larger elastic anomaly in C_{44} than

C_{66} . [12, 13] These works have implied the existence of diverse fluctuations in iron-based SCs. It will be an important object to investigate the relations between these fluctuations and their participation in the superconductivity. In this article, we will report all the elastic constants of $\text{Ba}(\text{Fe}_{1-x}\text{Co}_x)_2\text{As}_2$ with eight Co-concentrations to investigate the structural fluctuation with different symmetries in this system. We also report the diverse fluctuations inherent in iron-based superconductors.

2 Elastic constant measurement

2.1 Experimental Procedure

The elastic constant measurement was performed by an ultrasonic pulse-echo phase comparison method [14] as a function of temperature where the temperature ranged from 5 to 300 K. The temperature was controlled using a cryostat mounted on a Gifford-McMahon (GM) cryocooler. To prevent the damage to the sample due to rapid changes in temperature, the rate of change in temperature was carefully controlled so as to be 10 K/h near T_S [15].

Elastic stiffness was obtained by $C = \rho v^2$, where ρ is the density and v is either the longitudinal or transverse sound velocity, ρ was calculated by the lattice constant. Under the assumption of Vegard's law, the lattice constants of the a (b)- and c -axes are calculated by the data of $x = 0$ and 0.1 of $\text{Ba}(\text{Fe}_{1-x}\text{Co}_x)_2\text{As}_2$ to be $a = b = 0.39636 + 3.8981 \times 10^{-4}x$ (nm) and $c = 1.3022 - 0.0421x$ (nm), respectively. [16] The corresponding longitudinal or transverse sound velocity is obtained by choosing the propagation and displacement directions. In tetragonal crystal symmetry, we can measure six C_{ij} s; namely, C_{11} , C_{33} , C_{12} , C_{13} , C_{44} , and C_{66} . The propagation and displacement directions of the sound velocity are respectively [100] and [100] for C_{11} , [001] and [001] for C_{33} , [100] and [010] for C_{66} , [100] and [001] for C_{44} , [110] and $[\bar{1}\bar{1}0]$ for $\frac{1}{2}(C_{11} - C_{12})$, and [110] and [110] for $C_L = \frac{1}{2}(C_{11} + C_{12} + 2C_{66})$. Here, the XYZ coordinate was defined by the unit cell of the $I4/mmm$ crystal structure [17], where the directions of X , Y and Z coincide with the principal axes of base-centered tetragonal lattice formed by Ba atoms, which is indicated in Fig. 1. Absolute value of the sound velocity was obtained by the time interval of the echo train and the sample length, whose accuracy is within a few percent, dependent on the sample size.

For the velocity measurements, ultrasound was emitted and detected using LiNbO_3 transducers. Z -cut LiNbO_3 with 100 μm thickness was used for longitudinal ultrasonic waves, and a 41° X -cut plate of LiNbO_3 with 100 μm thickness was used for transverse waves. The fundamental frequencies of the longitudinal and transverse transducers were 33 and 19 MHz, respectively. In this experiment, a third-higher harmonics of 114 and 64 MHz were applied to generate the longitudinal and transverse sound waves, respectively. High-quality large single crystals of $\text{Ba}(\text{Fe}_{1-x}\text{Co}_x)_2\text{As}_2$ used in this work were grown by the self-flux method. Samples with eight Co-concentrations $x = 0, 0.037, 0.060, 0.084, 0.098, 0.116, 0.161,$ and 0.245 were prepared, and their corresponding compositions are shown in Fig. 1. The Co-concentration in the grown crystals was determined by energy-dispersive X-ray spectroscopy (EDS). Two samples were prepared for $x = 0.060$, which are abbreviated as sample B and D. [18] The samples were cut into a rectangular shape, after determining their axis by X-ray Laue photograph. The samples have an average typical area of $3 \times 3 \text{ mm}^2$ in the tetragonal ab (XY) cleavage plane, and

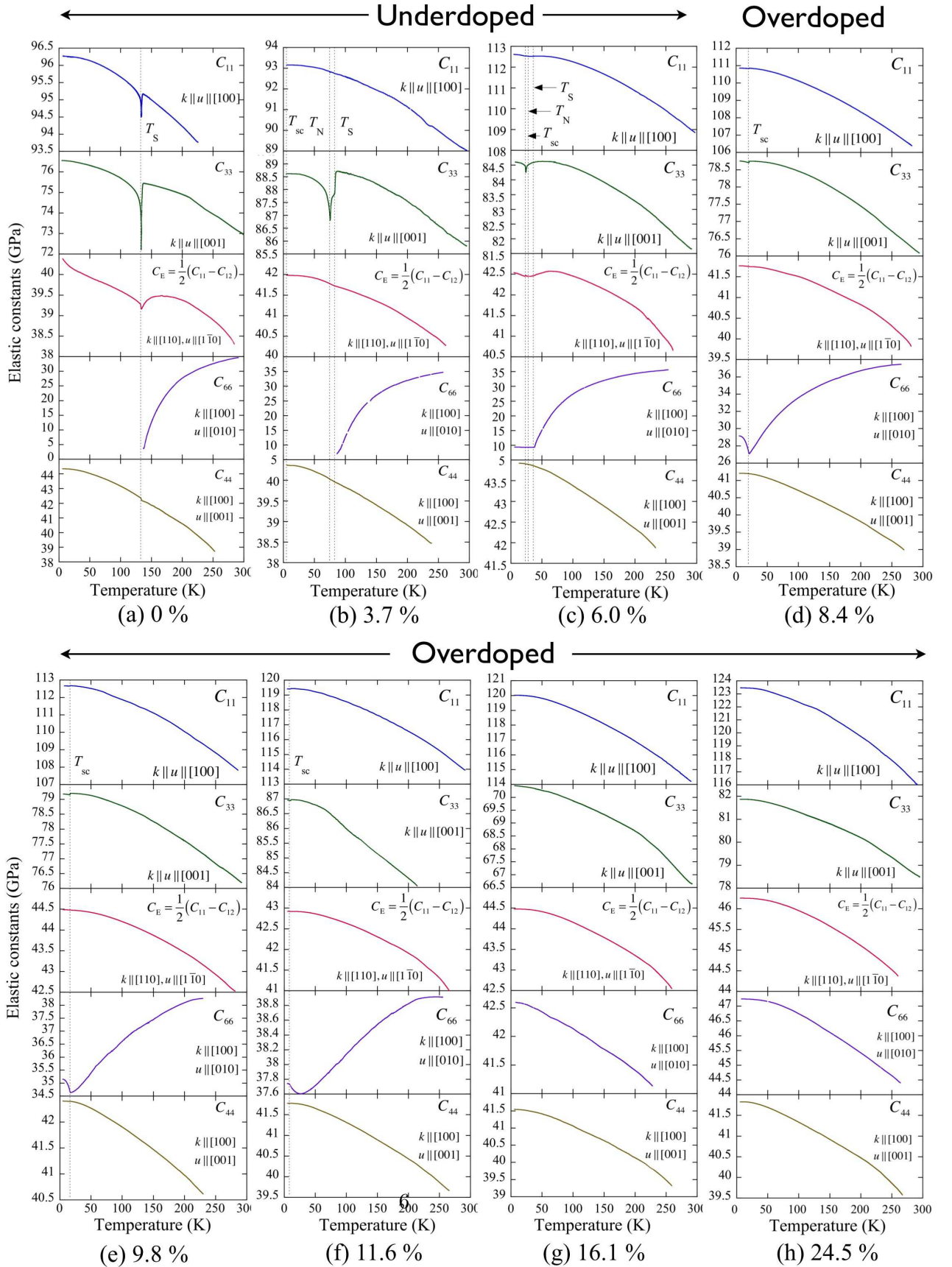


Figure 3: (Color online) Temperature-dependence of the elastic stiffness constants C_{11} , C_{33} , $C_E = (C_{11} - C_{12})/2$, C_{66} and C_{44} of $\text{Ba}(\text{Fe}_{1-x}\text{Co}_x)_2\text{As}_2$ with (a) $x = 0$, (b) $x = 0.037$, (c) $x = 0.060$, (d) $x = 0.084$, (e) $x = 0.098$, (f) $x = 0.116$, (g) $x = 0.161$ and (h) $x = 0.245$.

thickness of 2 mm on the $c(Z)$ -axis.

Recently, Kurihara *et al.* reported remarkable anomalies of ultrasonic attenuation coefficient for the same Co-doped Ba122 system. [19] We have measured ultrasonic attenuation in addition to sound velocity, and observed ultrasonic attenuation anomalies in some elastic modes and samples.[18] The results on the ultrasonic attenuation are not included in this article, because we have not made the systematic study.

3 Experimental Results

3.1 Underdoped region

The measured temperature dependence of elastic constants C_{ij} for all eight samples are summarized in Fig. 3. From the Fig. 3 we know that the parent compound BaFe₂As₂ shows remarkable elastic softening associated with the structural phase transition $T_S = 134$ K in C_{11} , C_{33} and C_{66} . C_{44} increases with decreasing temperature and show a small anomaly at T_S . C_E also shows remarkable anomaly at around T_S . In our previous paper, the large elastic softening in C_{66} of Ba122 was presented. In that discussions, the temperature dependence of C_{66} was characterized by a Jahn-Teller formula that corresponds to a Curie-Weiss expression for the magnetic susceptibility.[4]

On the other hand, as illustrated in Fig. 4, C_{11} (a) C_{11} and C_{33} show step-like temperature dependence, which comes from a magneto-elastic coupling between the structural and magnetic order parameters η and the elastic strain ε with the form of $\eta^2\varepsilon$. Also it can be seen from the Fig. 4, C_{11} (a) that C_{11} shows a hysteresis at low temperatures and it is dominated near the T_N and T_S . This hysteresis appearing in C_{11} implies that the structural transition is considered to be the first order. The elastic softening observed in C_{11} for parent compound BaFe₂As₂ did not appeared in Co = 3.7% sample. However, C_{33} shows elastic softening at two successive transition temperatures T_N and T_S . The details are shown in Fig. 4.

3.2 Near optimal concentration

For Co = 6.0 % sample which is near the optimal concentration, we have already reported precise temperature dependence of C_{66} and C_{33} [4, 18] and discussed in details about the elastic softening. From these results, it is remarkable that C_{33} shows an elastic softening towards T_N . As shown in Fig. 5, C_{11} also shows a slight elastic softening at around 20 K in addition to the elastic softening in C_{33} . Superconducting transition is observed in both C_{11} and C_{33} . It is interesting that C_{11} shows a small anomaly at around T_{sc} , however any anomaly observed at T_N , but C_{33} shows a remarkable elastic softening towards T_N and T_{sc} . Since the C_{33} anomaly can be analyzed by Jahn-Teller formula, the elastic softening of C_{33} would be ascribed to orbital fluctuations of inter-layer $O_{3z^2-r^2}$. Thus, our results suggest the coexistence of different kinds of orbital fluctuations, in addition of O_{xy} appearing in C_{66} . Recently, a two-dome structure has been reported in the superconducting transition of 1111 system LaFeAsO_{1-x}H_x. [20] On the origin of the superconductivity of this system, the important role of $O_{3z^2-r^2}$ orbital has been discussed.[20, 21] By considering the above research results, we suppose that various fluctuations exist inherently in Ba122 system and play important role in the emergence of superconductivity.

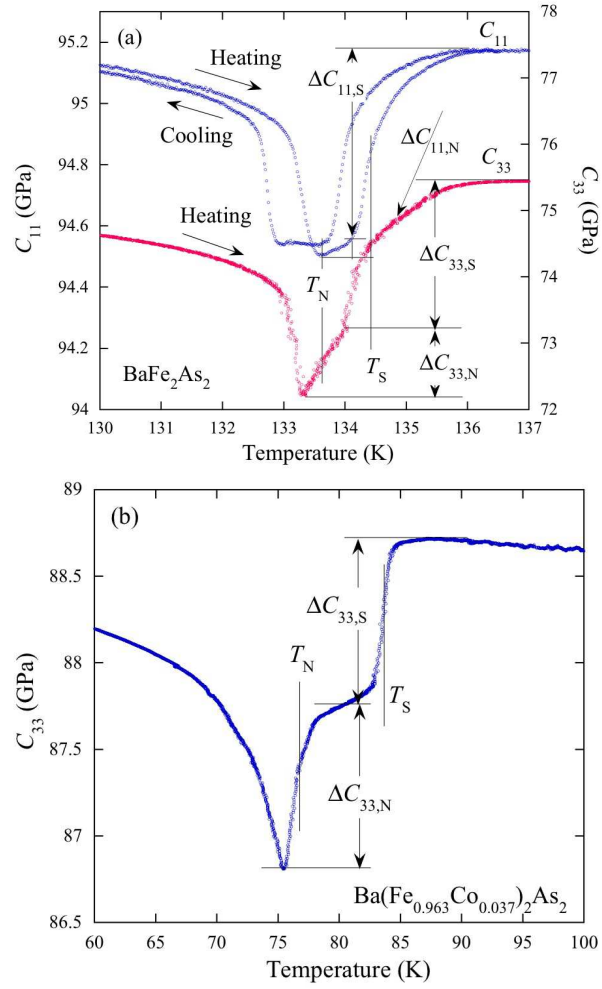


Figure 4: (Color online) (a) Temperature dependence of C_{11} and C_{33} in BaFe_2As_2 , and (b) C_{33} in $\text{Ba}(\text{Fe}_{0.963}\text{Co}_{0.037})_2\text{As}_2$.

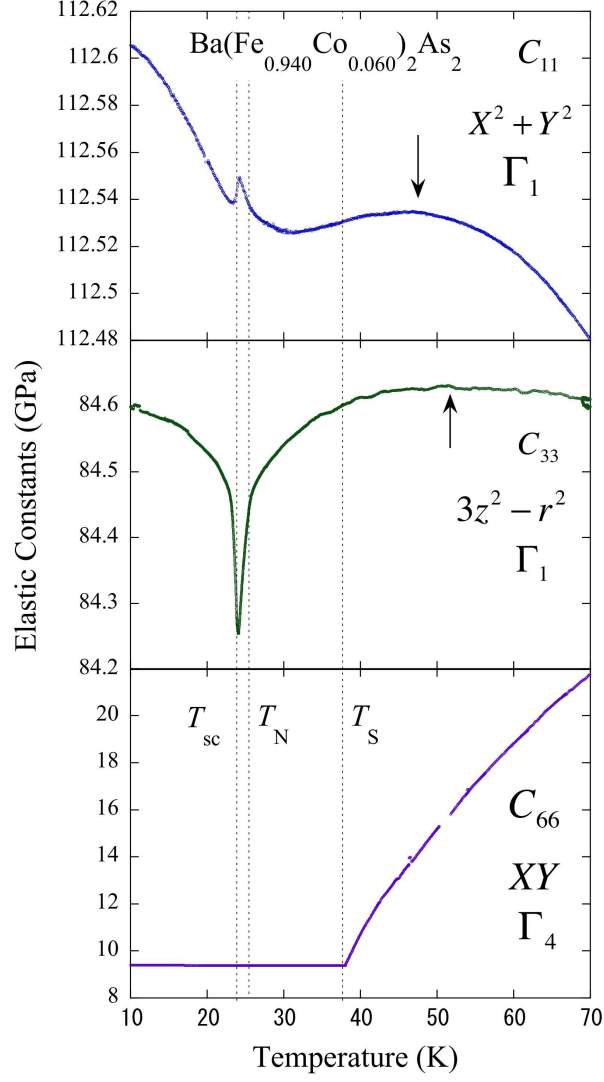


Figure 5: (Color online) Temperature dependence of C_{11} , C_{33} and C_{66} . Their irreducible representations and bases are Γ_1 and $X^2 + Y^2$ for C_{11} , Γ_1 and $3z^2 - r^2$ for C_{33} , and Γ_4 and XY for C_{66} . T_S is observed in sole C_{66} . On the other hand, T_N and T_{sc} are apparent in C_{11} and C_{33} , which are followed by elastic softening from high temperatures.

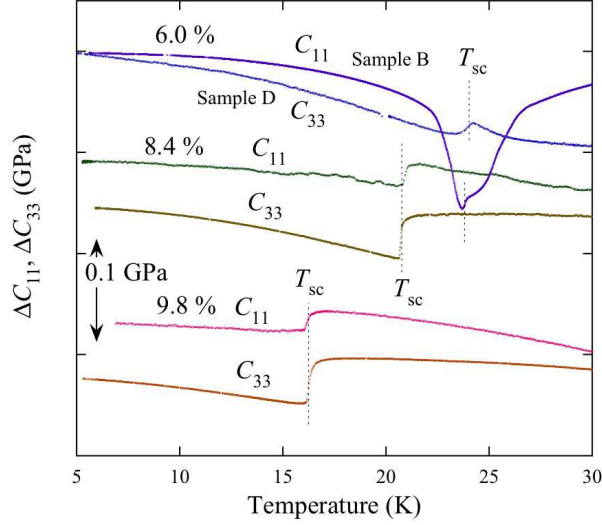


Figure 6: (Color online) Temperature dependence of C_{11} and C_{33} for 6.0 %, 8.4 % and 9.8 % samples. C_{11} data for 6.0 % sample were taken from the sample B, and C_{33} from the sample D, because the sample B does not show apparent anomaly at T_{sc} in C_{33} .

Here, we have to remark an important fact on the phase diagram. The difference between T_S and T_N is 1 K for BaFe_2As_2 , 10 K for $\text{Co} = 3.7\%$ sample, and 12 K for $\text{Co} = 6.0\%$ sample. The difference between T_S and T_N becomes larger with increasing the Co-concentration. This behavior differs from the case of BaNi_2As_2 , where T_S and T_N tends to merge by approaching the optimal concentration. The experimental result of BaNi_2As_2 has been discussed from the point of avoided quantum criticality.[22]

3.3 Overdoped region

Overdoped samples show rather monotonous temperature dependence in all elastic constants except C_{66} . Elastic anomalies associated with T_{sc} were observed in all elastic constants. In over-doped region, the elastic softening in C_{66} above T_{sc} tends to disappear with the increase of Co-concentration. As shown in Fig. 6, C_{11} and C_{33} show step-like anomalies at T_{sc} , which are caused by a magneto-strictive coupling between the superconducting order parameter and the elastic strain.

4 Discussion

4.1 Grüneisen Parameter

In this section, we will discuss about the Grüneisen parameters for the structural transition temperature T_S , the magnetic transition temperature T_N , and the superconducting transition temperature T_{sc} . Grüneisen parameter is a measure of the interaction between order parameter and strain via magneto-strictive coupling, which

Table 1: Anomalous part of C_{11} and C_{33} at T_S ($\Delta C_{11,S}$ and $\Delta C_{33,S}$), specific heat anomaly at T_S ($\Delta C_{p,S}$), and the absolute values of calculated Grüneisen parameters $|\Omega_{a,S}|$ and $|\Omega_{c,S}|$ for BaFe₂As₂, the 3.7%, and 6.0%-doped samples. Anomalous part of C_{11} and C_{33} at T_N ($\Delta C_{11,N}$ and $\Delta C_{33,N}$), specific heat anomaly at T_N ($\Delta C_{p,N}$), and the absolute values of calculated Grüneisen parameters $|\Omega_{a,N}|$ and $|\Omega_{c,N}|$ for BaFe₂As₂, the 3.7%, and 6.0%-doped samples. Specific heat data were taken from Simayi *et al.*[18] and unpublished data. *1) No precise measurement, but it would be concluded to be very small from rough measurements.

x -Co (%)	0	3.7	6.0
T_S (K)	134.4	83.7	37.5
$\Delta C_{11,S}$ (GPa)	-0.62	0	0
$\Delta C_{33,S}$ (GPa)	-2.27	-0.95	0
$\Delta C_{p,S}$ (mJ/mol·K)	3.0	0.6	*1
$ \Omega_{a,S} $	2.3	0	—
$ \Omega_{c,S} $	4.4	12.9	—
T_N (K)	133.6	76.8	25.7
$\Delta C_{11,N}$ (GPa)	-0.057	0	0
$\Delta C_{33,N}$ (GPa)	-1.00	-0.93	0.21
$\Delta C_{p,N}$ (mJ/mol·K)	8.8	1.55	≈ 0
$ \Omega_{a,N} $	0.4	0	—
$ \Omega_{c,N} $	1.8	9.0	—

can be described by Eq. (1). We could obtain the absolute value of the Grüneisen parameter Ω experimentally from the specific heat jump ΔC_V (we used C_p instead of C_V) and the elastic constant jump ΔC at the transition temperature (T_C) by using the following formula.

$$\Omega = -\frac{1}{T_C} \frac{\partial T_C}{\partial \varepsilon} \quad \text{and} \quad \Delta C = -\Omega^2 \Delta C_V T_C \quad (1)$$

Here, ε is the elastic strain.

At first, we will calculate the Grüneisen parameter for T_S and T_N by using Eq. (2). The data used for the calculation are listed in Table I, and the Co-concentration dependence is shown in Fig. 7.

$$\Omega_{a,S} = -\frac{1}{T_S} \frac{\partial T_S}{\partial \varepsilon_{XX}} \quad \text{and} \quad \Delta C_{11,S} = -\Omega_{a,S}^2 \Delta C_{p,S} T_S, \quad (2a)$$

$$\Omega_{c,S} = -\frac{1}{T_S} \frac{\partial T_S}{\partial \varepsilon_{ZZ}} \quad \text{and} \quad \Delta C_{33,S} = -\Omega_{c,S}^2 \Delta C_{p,S} T_S, \quad (2b)$$

$$\Omega_{a,N} = -\frac{1}{T_N} \frac{\partial T_N}{\partial \varepsilon_{XX}} \quad \text{and} \quad \Delta C_{11,N} = -\Omega_{a,N}^2 \Delta C_{p,N} T_N, \quad (2c)$$

$$\Omega_{c,N} = -\frac{1}{T_N} \frac{\partial T_N}{\partial \varepsilon_{ZZ}} \quad \text{and} \quad \Delta C_{33,N} = -\Omega_{c,N}^2 \Delta C_{p,N} T_N. \quad (2d)$$

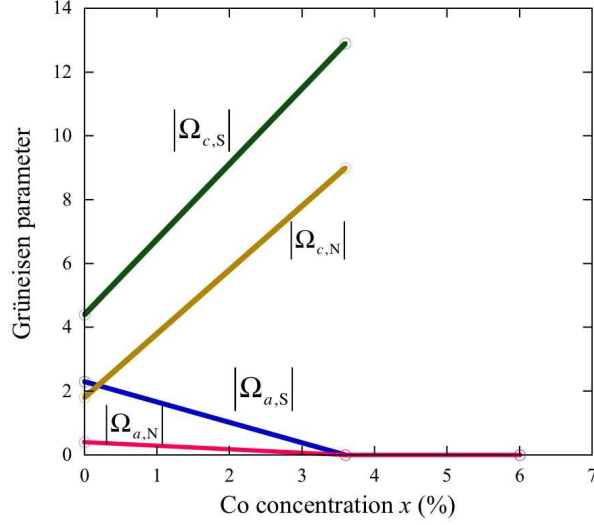


Figure 7: (Color online) Co-concentration dependence of Grüneisen parameters Ω_S and Ω_N .

$\Omega_{c,S}$ and $\Omega_{c,N}$ increase towards the QCP, while $\Omega_{a,S}$ and $\Omega_{a,N}$ tend to be zero as approaching QCP. For the Co = 6.0 % sample, no specific heat anomaly was found at T_N and T_S , because the temperature was roughly scanned near these transition temperatures. We suppose, however, they are very small. It may imply that both Grüneisen parameter $\Omega_{c,S}$ and $\Omega_{c,N}$ are considered to be quite large for 6.0 %, and would show divergent behavior towards QCP. According to the recent works, the Grüneisen parameter is expected to be divergent near the QCP.[23, 24] Although the iron-based superconductors show in-plane structural and magnetic orders, however the calculated Grüneisen parameters in this study related to the inter-plan direction show a relevant Grüneisen parameters. Next, Grüneisen parameters for T_{sc} were evaluated by the same manner by using Eq.(3) and the data listed in Table II.

$$\Omega_a = -\frac{1}{T_{sc}} \frac{\partial T_{sc}}{\partial \varepsilon_{XX}} \quad \text{and} \quad \Delta C_{11,sc} = -\Omega_a^2 \Delta C_{p,sc} T_{sc}, \quad (3a)$$

$$\Omega_c = -\frac{1}{T_{sc}} \frac{\partial T_{sc}}{\partial \varepsilon_{ZZ}} \quad \text{and} \quad \Delta C_{33,sc} = -\Omega_c^2 \Delta C_{p,sc} T_{sc}. \quad (3b)$$

The values of Ω_c were already reported in the previous paper.[18] In addition to Ω_c , we evaluated Ω_a in this work. We cannot determine the sign of Ω_a and Ω_c from the elastic constant measurement. Some hypothesis or careful consideration will be needed to determine their sign. We will discuss later on this point.

Here, we will compare our results with those of previous thermal expansion measurements. For comparison, we should convert our results as a function of the uniaxial strain dependence $dT_{sc}/d\varepsilon_i$ to that of the uniaxial pressure dependence of

T_{sc} by using the following formulas:

$$\frac{dT_{sc}}{d\varepsilon_{XX}} = -(C_{11} + C_{12}) \frac{dT_{sc}}{dp_a} - C_{13} \frac{dT_{sc}}{dp_c}, \quad (4a)$$

$$\frac{dT_{sc}}{d\varepsilon_{ZZ}} = -C_{33} \frac{dT_{sc}}{dp_c} - 2C_{13} \frac{dT_{sc}}{dp_a}. \quad (4b)$$

The values of 109, 79, and 29 GPa were used for C_{11} , C_{33} , and C_{12} respectively. In this calculation, it was assumed that C_{13} is the same value as C_{12} because C_{13} was not measured and is unknown. Bud'ko *et al.* reported dT_{sc}/dp_i for 3.8% and 7.4%, and Hardy *et al.* reported dT_{sc}/dp_i for 8.0%. We compare these values of $\frac{dT_{sc}}{d\varepsilon_{XX}}$ obtained by our measurements with those calculated by using the reported values of $\frac{dT_{sc}}{dp_a}$ and $\frac{dT_{sc}}{dp_c}$. Hardy *et al.* obtained $dT_{sc}/dp_a = 3.1(1)$ K/GPa and $dT_{sc}/dp_c = -7.0(2)$ K/GPa for 8% doped sample from the thermal expansion measurement.[25] The value of dT_{sc}/dp_c is comparable to that by Nakashima *et al.* of -13 K/GPa for 8% doped sample.[26] These values give the Ω_a and $dT_{sc}/d\varepsilon_{XX}$ to be 10.0 and -219 K, and Ω_c and $dT_{sc}/d\varepsilon_{ZZ}$ to be -16.7 and 365 K, respectively, for 8% doped sample. These values are consistent with our results of $|\Omega_a| = 11.2$ and $|\Omega_c| = 16.2$ for the 8.4 % doped sample.

On the other hand, Bud'ko *et al.* reported $dT_{sc}/dp_a = -4.1$ K/kbar and $dT_{sc}/dp_c = 1.7$ K/kbar for 3.8% doped sample, $dT_{sc}/dp_a = 0.3$ K/kbar and $dT_{sc}/dp_c = -2.6$ K/kbar for 7.4% doped sample [27]. Grüneisen parameters for the 7.4 % sample are $\Omega_a = -14.2$ and $\Omega_c = -91.6$, which are remarkably different from our results. Origin of the inconsistency between our results and Bud'ko's ones is an enigma.

Next, we have to pay our attention to the sign of the Grüneisen parameter. We try to determine their sign from the information of thermal expansion data. We were aware of some tendency in the dT_{sc}/dp_a and dT_{sc}/dp_c as a function of Co-concentration in the previous thermal expansion measurements. dT_{sc}/dp_c is positive for underdoped samples, and negative for the overdoped doped samples.[27] dT_{sc}/dp_a has an opposite sign of dT_{sc}/dp_c . [25] The decrease of T_{sc} was reported by the uniaxial pressure along c -axis for an overdoped sample.[26] These results suggest that the sign of Ω_a and Ω_c are negative and positive, respectively, in the underdoped region, and vice versa in overdoped region. Therefore, we assumed that sign of the Grüneisen parameters follows along a general tendency observed in the previous works, and listed in Table II.

Figure 8 shows the Co-concentration dependence of Ω_{sc} . The calculated Grüneisen parameters in this study have been plotted with the data from Hardy *et al.* and Drotziger *et al.*[25, 28] To compare our results with those of Drotziger *et al.*, we evaluated $\partial T_{sc}/\partial P$ from their article, and obtained by the formula of $(C_B/T_{sc})(\partial T_{sc}/\partial P)$. Here, C_B is the bulk modulus, which was evaluated to be 44 GPa by using

$$C_B = \frac{(C_{11} + C_{12})C_{33} - 2C_{13}^2}{C_{11} + 2C_{33} + C_{12} - 4C_{13}}, \quad (5)$$

under the assumption of $C_{13} = C_{12}$. In the case of Hardy's result, the sign of Ω obtained by the formula $\Omega = 2\Omega_a + \Omega_c$ is positive, and that obtained by $(C_B/T_{sc})(\partial T_{sc}/\partial P)$ is negative. This inconsistency was considered to be caused by the values of the elastic constants used in Eqs. (3) and (4). We consider that the sign of the Grüneisen parameters alternate with the opposite one near the QCP. If the hydrostatic pressure was applied, the sign of $\partial T_{sc}/\partial P$ is positive for the underdoped samples and negative

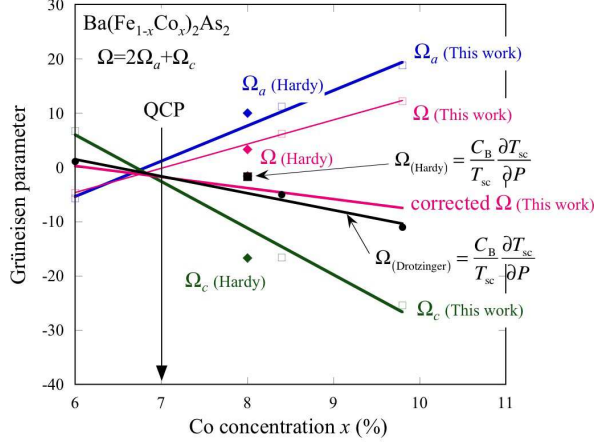


Figure 8: (Color online) Co-concentration dependence of Grüneisen parameter Ω_{sc} .

Table 2: T_{sc} , ΔC_{33} , $\Delta C_p/T_{sc}$, dT_{sc}/dp_c , calculated $dT_{sc}/d\varepsilon_{ZZ}$, and Ω values for the 6.0%-, 8.4%-, and 9.8%-doped samples. Specific heat data were taken from Simayi *et al.*[18] and unpublished data.

x -Co (%)	6.0	8.4	9.8
T_{sc} (K)	24.0	20.6	16.7
$\Delta C_{11,sc}$ (10^{-2} GPa)	-1.0	-2.0	-2.4
$\Delta C_{33,sc}$ (10^{-2} GPa)	-1.4	-4.2	-4.4
$\Delta C_{p,sc}$ (mJ/mol·K)	792	474	251
Ω_a	-5.7	11.2	18.8
Ω_c	6.7	-16.2	-25.2
Ω	-4.7	6.2	12.4

for the overdoped samples. It would be reasonable, because T_{sc} shows a maximum near the QCP, which results that T_{sc} is not influenced by the change of any external parameter. This means that the bulk Grüneisen parameter Ω should be approximately zero near the QCP. In our original data, Ω is negative for the underdoped region and positive for the over-doped region, and it increases with the increasing of Co-concentration, it would be somewhat unreasonable. As the same reason as the inconsistency in the Hardy's result, if we try to change the values of Ω_a and Ω_c by multiplying some coefficients; namely, $0.7\Omega_a$, $1.3\Omega_c$ and $\Omega_{corrected} = 0.7\Omega_a + 1.3\Omega_c$, $\Omega_{corrected}$ takes positive sign in underdoped region and negative sign in overdoped region and shows similar behavior to Drotzinger *et al.*[28] We plotted these Grüneisen parameters as a function of Co-concentration in Fig. 8.

In this section, the Grüneisen parameters have been calculated for for T_S , T_N and T_{sc} as a function of Co-concentration. T_S and T_N are not affected by in-plane elongation and compression, but did not affected by in-plane elongation and compression. These findings in this work is very striking, because it has been believed that structural and magnetic orders are quasi-2-dimensional and sensitive to in-plane

deformation. On the other hand, from the above results we know that in-plane contraction and inter-plane elongation enhance T_{SC} . In particular, the c -axis elongation stabilizes the superconductivity. The same deformation also promote the structural and magnetic orders. These facts suggest that the existence of certain correlation between the structural and magnetic orders and superconductivity. Γ_1 fluctuation appearing in C_{33} plays an important role in the emergence of superconductivity in addition to in-plane C_{66} fluctuations.

4.2 Elastic anomaly associated with superconductivity

In this subsection, we will focus our attention on the elastic anomaly associated with the superconductivity. It has been reported that the elastic anomaly in C_{66} at T_{sc} is quite different between underdoped and overdoped regions. In the underdoped region, C_{66} shows an elastic hardening at T_{N} , and shows softening at T_{sc} . [4] On the other hand, C_{66} increases with an up-turn at T_{sc} followed by a large elastic softening. [9, 4] This behavior ascribed to the phase transition in tetragonal phase (overdoped case) and orthorhombic phase (underdoped case). In other words, we suppose that it would be a signature that superconductivity of both cases are qualitatively different from each other.

For the overdoped region, Fig. 9(a) is the temperature dependence of C_{66} for 8.4 % and 9.8 % samples. Bold lines above T_{sc} are the theoretical fit by using the following equations, taking the band contribution into account, which were precisely reported elsewhere. [4]

The elastic anomaly associated with band electrons is described by the following charge susceptibility.

$$\chi_s = - \int dE N(E) \frac{\partial f(E)}{\partial E} \quad (6)$$

where f and N the Fermi-Dirac function and the density of states.

The curves below T_{sc} in Fig. 9(a) are guides for eyes. According to Eq.(6), the elastic anomaly by the band electron is considered to vanish associated with a gap opening in the superconducting phase, because N_0 is zero below T_{sc} . This makes C_{66} increase below T_{sc} . From this consideration, the amount of elastic anomaly above T_{sc} (ΔC_n) is expected to be equal to that below T_{sc} ($-\Delta C_s$) at $T = 0$ K, because the density of states at Fermi energy is zero for a full-gap SCs.

In Fig. 9(b) shows the plotted ΔC_n as a function of $-\Delta C_s$ for 8.4 %, 9.8 % and 11.6 % samples. We found two peculiar behaviors from the figure. First, the relation of $\Delta C_s = -\Delta C_n$ does not hold. The ratio of ΔC_s against $-\Delta C_n$ was evaluated to be 0.28 from the tendency of the three samples, which is indicated by the straight line in Fig. 9(b). If the elastic anomaly in the normal phase would be contributed solely by the band, than the band with a gap opened is 28 % of the band responsible for the elastic softening. The rest of 72 % is considered to be gapless, or does not participate in the superconductivity. Second, ΔC_s vanishes more steeply than $-\Delta C_n$ with increasing Co-concentration. ΔC_s reaches to zero when $-\Delta C_n = 10$ GPa. The second finding is that ΔC_s decreases rapidly and almost zero for 11.6 % sample, although its $T_{\text{sc}} = 10.5$ K.

These phenomena are very peculiar, and the origin is an enigma. However, it should be remark that these discussions in this work are considered to be valid for

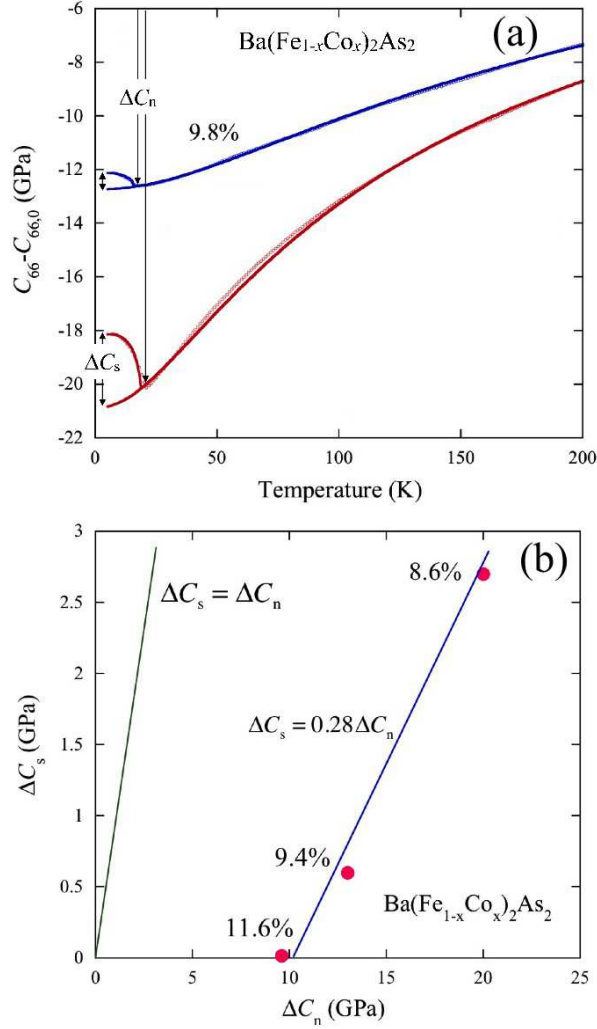


Figure 9: (Color online) (a) Temperature dependence of C_{66} and. Bold lines above T_{sc} are the calculation taken from the previous study.[4]. The curves below T_{sc} are the guides for eyes. (b) Anomaly associated with superconductivity ΔC_s as a function of the elastic anomaly in the normal phase $\Delta C_n (= C_{66} - C_{66,0}$ at T_{sc}).

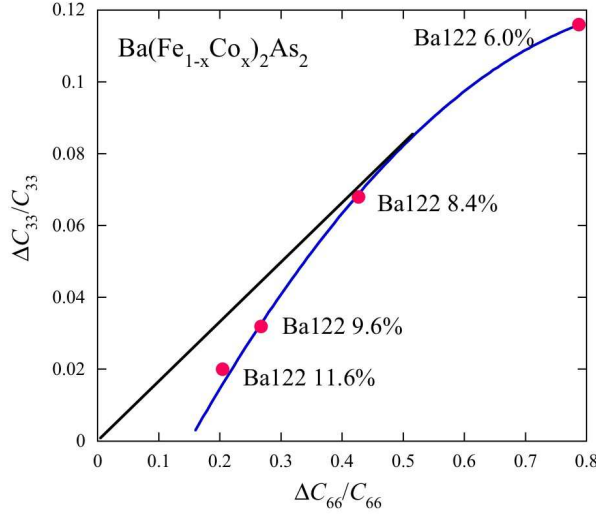


Figure 10: (Color online) Temperature dependence of C_{11} , C_{33} and C_{66} .

typical s_{++} full-gap SCs. Therefore, the origin of these behavior should be carefully discussed, and will remain as a future task.

5 Conclusion

In this work, total 40 elastic constants with five elastic modes of C_{11} , C_{33} , $C_E = (C_{11} - C_{12})/2$, C_{44} and C_{66} for $\text{Ba}(\text{Fe}_{1-x}\text{Co}_x)_2\text{As}_2$ (where $x = 0, 3.7, 6.0, 8.4, 9.8, 11.6, 16.1$ and 24.5) single crystalline samples have been presented. We focused our attention on the elastic anomalies in C_{11} and C_{33} modes, and discussed Grüneisen parameters of this system. Although, some assumption for the determination of the sign for Grüneisen parameters were adopted, it would be considered that Grüneisen parameters of Ba122 system are very anisotropic. It would be accepted that the bulk Grüneisen Ω is zero near optimal concentration. Although our results surely indicate that both Ω_a and Ω_c are very small near the optimal concentration, they develop differently with leaving from the optimal concentration. The bulk Ω keeps nearly zero as a consequence of cancellation of Ω_a and Ω_c with an opposite sign. Owing to this property, T_{sc} could be stable against hydrostatic pressure, however the T_{sc} is expected to be enhanced by uniaxial pressure. Higher T_{sc} would be realized by contraction of ab -plane and expansion along c -direction by chemical treatment of replacing atoms.

This suggestion can be replaced by other word from the viewpoint of relevant role of structural fluctuation along c -axis, because c -axis elongation is preferable for $3z^2 - r^2$ orbital. In our previous paper, we pointed out anomalous softening in C_{33} near the optimal concentration.[18] Figure 5 shows that C_{11} anomaly exists in addition to C_{33} . C_{11} and C_{33} softening represent C_4 fluctuation. Figure 10 shows the amount of C_{33} softening as a function of the amount of C_{66} softening. There exists a correlation between the amount of C_{33} and C_{66} anomalies. While C_{66} expresses

C_2 fluctuation, C_{33} is C_4 fluctuation. Two types of fluctuations seem to cooperate near the QCP. It would be concluded that the superconductivity with high T_{sc} of this system is brought about by the collaboration of C_2 fluctuation and C_4 .

Acknowledgments

We would like to thank T. Kowata for his help in determining the atomic composition of the samples by using EDS. This work was supported by the Transformative Research-project on Iron Pnictides of the Japan Science and Technology Agency, JSPS KAKENHI Grant Number 24500350 and JP15H05883 (J-Physics).

5.1 A subsection

More text.

References

- [1] Y. Kamihara, T. Watanabe, M. Hirano, and H. Hosono: *J. Am. Chem. Soc.* **130** (2008) 3296.
- [2] D. C. Johnston: *Adv. Phys.* **59** (2010) 803.
- [3] L. Boeri, O. V. Dolgov, and A. A. Golubov: *Phys. Rev. Lett.* **101** (2008) 026403.
- [4] M. Yoshizawa, D. Kimura, T. Chiba, S. Simayi, Y. Nakanishi, K. Kihou, C. H. Lee, A. Iyo, H. Eisaki, M. Nakajima, and S. Uchida: *J. Phys. Soc. Jpn.* **81** (2012) 024604.
- [5] P. C. Canfield, S. L. Bud'ko, N. Ni, J. Q. Yan, and A. Kracher: *Phys. Rev. B* **80** (2009) 060501(R).
- [6] Y. Laplace, J. Bobroff, F. Rullier-Albenque, D. Colson, and A. Forget: *Phys. Rev. B* **80** (2009) 140501(R).
- [7] M. A. McGuire, A. D. Christianson, A. S. Sefat, B. C. Sales, M. D. Lumsden, R. Jin, E. A. Payzant, D. Mandrus, Y. Luan, V. Keppens, V. Varadarajan, J. W. Brill, R. P. Hermann, M. T. Sougrati, F. Grandjean, and G. J. Long: *Phys. Rev. B* **78** (2008) 094517.
- [8] R. M. Fernandes, L. H. VanBebber, S. Bhattacharya, P. Chandra, V. Keppens, D. Mandrus, M. A. McGuire, B. C. Sales, A. S. Sefat, and J. Schmalian: *Phys. Rev. Lett.* **105** (2010) 157003.
- [9] T. Goto, R. Kurihara, K. Araki, K. Mitsumoto, M. Akatsu, Y. Nemoto, S. Tatematsu, and M. Sato: *J. Phys. Soc. Jpn.* **80** (2011) 073702.
- [10] H. Kontani, T. Saito, and S. Onari: *Phys. Rev. B* **84** (2011) 024528.
- [11] H. Kontani, Y. Inoue, T. Saito, Y. Yamakawa, and S. Onari: *Solid State Commun.* **152** (2012) 718.
- [12] H. Takezawa, K. Sakano, S. Simayi, C. Fujii, M. Nakamura, Y. Nakanishi, Y. Koshika, Y. Takahashi, T. Watanabe, and M. Yoshizawa: *JPS Conf. Proc.* **3** (2014) 016025.

- [13] K. Horikoshi, J. Imai, Y. Nakanishi, M. Nakamura, T. Kobayashi, T. Adachi, S. Miyasaka, S. Tajima, and M. Yoshizawa: *Physica B* (2017) (in press).
- [14] B. Luethi: *Physical Acoustics in the Solid State* (Springer, Heidelberg, 2004), p. 9.
- [15] Q. Huang, Y. Qiu, W. Bao, M. A. Green, J. W. Lynn, Y. C. Gasparovic, T. Wu, G. Wu, and X. H. Chen: *Phys. Rev. Lett.* **101** (2008) 257003.
- [16] A. S. Sefat, R. Jin, M. A. McGuire, B. C. Sales, D. J. Singh, and D. Mandrus: *Phys. Rev. Lett.* **101** (2008) 117004.
- [17] M. Rotter, M. Tegel, D. Johrendt, I. Schellenberg, W. Hermes, and R. Pöttgen: *Phys. Rev. B* **78** (2008) 020503(R).
- [18] S. Simayi, K. Sakano, H. Takezawa, M. Nakamura, Y. Nakanishi, K. Kihou, M. Nakajima, C.-H. Lee, A. Iyo, H. Eisaki, S. ichi Uchida, and M. Yoshizawa: *J. Phys. Soc. Jpn.* **82** (2013) 114604.
- [19] R. Kurihara, K. Mitsumoto, M. Akatsu, Y. Nemoto, T. Goto, Y. Kobayashi, and M. Sato: *J. Phys. Soc. Jpn.* **86** (2017) 064706.
- [20] N. Fujiwara, S. Tsutsumi, S. Iimura, S. Matsuishi, H. Hosono, Y. Yamakawa, and H. Kontani: *Phys. Rev. Lett.* **111** (2013) 097002.
- [21] S. Onari, Y. Yamakawa, and H. Kontani: *Phys. Rev. Lett.* **112** (2014) 187001.
- [22] X. Lu, H. Gretarsson, R. Zhang, X. Liu, H. Luo, W. Tian, M. Laver, Z. Yamani, Y.-J. Kim, A. H. Nevidomskyy, Q. Si, and P. Dai: *Phys. Rev. Lett.* **110** (2013) 257001.
- [23] L. Zhu, M. Garst, A. Rosch, and Q. Si: *Phys. Rev. Lett.* **91** (2003) 066404.
- [24] R. Küchler, P. Gegenwart, F. Weickert, N. Oeschler, T. Cichorek, M. Nicklas, N. Carocca-Canales, C. Geibel, and F. Steglich: *Physica B* **378-380** (2006) 36.
- [25] F. Hardy, P. Adelman, T. Wolf, H. v. Löhneysen, and C. Meingast: *Phys. Rev. Lett.* **102** (2009) 187004.
- [26] Y. Nakashima, H. Yui, and T. Sasagawa: *Physica C* **470** (2010) 1063.
- [27] S. L. Bud'ko, N. Ni, S. Nandi, G. M. Schmiedeshoff, and P. C. Canfield: *Phys. Rev. B* **79** (2009) 054525.
- [28] S. Drotziger, P. Schweiss, K. Grube, T. Wolf, P. Adelman, C. Meingast, and H. v. Löhneysen: *J. Phys. Soc. Jpn* **79** (2010) 124705.